NIR Nanoterminator with Mature Dendritic Cell Acitivities for Immuno-Priming Mild Photothermal Cancer Therapy

Zhihong Sun[‡], Guanjun Deng[‡], Xinghua Peng[‡], Xiuli Xu, Lanlan Liu, Zhen Xu, Yifan Ma, Pengfei Zhang,[*] Ping Gong,[*] and Lintao Cai[*]

Z Sun, Dr. G Deng, X. Peng, L Liu, Dr. Z Xu, Prof. Y Ma, Prof. P. Zhang, Prof. P. Gong, Prof. L Cai

Guangdong Key Laboratory of Nanomedicine, Shenzhen Engineering Laboratory of Nanomedicine and Nanoformulations, CAS-HK Joint Lab for Biomaterials, CAS Key Laboratory of Health Informatics, Institute of Biomedicine and Biotechnology, Shenzhen Institutes of Advanced Technology, Chinese Academy of Sciences, Shenzhen, 518055, China
E-mail: lt.cai@siat.ac.cn
E-mail: pf.zhang@siat.ac.cn
Prof. P. Gong
Dongguan Key Laboratory of Drug Design and Formulation Technology, Key Laboratory for Nanomedicine, Guangdong Medical University, Dongguan 523808, China.
E-mail: ping.gong@siat.ac.cn
X Xu
Nano Science and Technology Institute, University of Science &Technology of China, Suzhou. 215123, P. R. China.
L Liu
University of Chinese Academy of Sciences, Beijing 100049, P. R. China
Prof. Y Ma
HRYZ Biotech Co. Shenzhen 518057, P. R. China
‡ These authors contributed equally to this work
Corresponding Authors
*E-mail: lt.cai@siat.ac.cn.
*E-mail: ping.gong@siat.ac.cn
*E-mail: pf.zhang@siat.ac.cn

Keywords: NIR, mild photothermal therapy, mature dendritic cells, tumor-immune microenvironment, biomimetic theranostics

Abstract:
Recently, photothermal-immuno synergistic therapy under mild temperature (~ 45 °C) has got broad interest in cancer treatment. Inhibition the intratumorally HSPs production is the key to accomplish highly efficient and mild photothermal therapy. In this work, we developed biomimetic nanoterminators with mature DCs functions by coating the mature dendritic cell membrane on photothermal nanoagents. As-prepared nanoterminators could automatically locate on T cell in the complex tumor-immune microenvironment and promote the T cells proliferation, activation and cytokine secretion, which could not only inhibit the expression of heat shock proteins to cooperate on highly efficient mild photothermal therapy (~42°C), but also promote tumor apoptosis during the treatment. More importantly, this nanoterminator could serve as vaccine to trigger anti-tumor immune response of the whole body, which would be promising to long-life tumor inhibition and termination.

Cancer has become the leading cause of death with the morbidity and mortality still rising and posed a serious threat to public health. [1] Photothermal therapy (PTT) has emerged as a promising light-based therapeutic paradigm toward precise cancer therapy due to its advantages of localized treatment, noninvasiveness, and controllable irradiation. [2] In this therapy, photothermal agents with near-infrared absorbing ability in the target tissue under irradiation can cause local temperature elevation because they can convert the incident light into heat. [3] Typically, rigorous photothermal heating to high temperature over 50 °C is required to achieve a relatively harsh environment for efficient ablation of tumors. However, the high temperature will transfer heat to surrounding normal tissues, killing them along with the tumor cells. In this situation, mild photothermal therapy with a relatively low temperature at ~ 45 °C has been proposed for tumor treatment. [4] Unfortunately, such a small elevation in temperature can stimulating the self-protection and self-repairing activity of tumor cells with the help of heat shock proteins (HSPs). HSPs were molecular chaperone for repairing the heat-denatured proteins, which overexpress in multiple tumors and played a key role in tumor thermoresistance. As a result, inhibition the intratumorally HSPs production is the key to accomplish highly efficient and mild photothermal therapy. [4b,5]

Cancer immunotherapy exploits the body's own immune system to fight against cancer [6]. When galvanized, the immune system is an extremely potent force that can mediate not only robust killing of cancer cells but also life-long autoimmunity. [6b, 7] T cells in the immune system, which protect the human body from infection by

pathogens and clear mutant cells through specific recognition by T cell receptors (TCRs) have been shown to have a crucial role in immunotherapy. Unfortunately, tumors are poorly immunogenic, and T-cell proliferation to self-antigens is tightly controlled, with self-reactive T cells being relatively non-responsive or completely absent [6c, 9]. As a result, T cells fail to proliferate and persist in response to tumors. It is highly desired to develop alternative approach to increase the antitumor potential of T cells in situ. [10]

Dendritic cells (DC) are “professional” antigen-presenting cells (APC) that can prime T cells. [11] Many studies suggest that mature DCs could induce potent antitumor T cell immunity [11b,12]. The priming of T cells by mature DCs was mainly through cell membrane surface components (such as MHC-antigen peptide complex, CD80/B7-1, CD86/B7-2, CD40, etc.), which may be important for highly functional therapeutic T cells generation. [13] The dendritic cells promote T cells to directly kill tumors or secrete cytokines (TNF-α, IL-2, and IFN-γ) to remove the tumor. [13b,14] Tumor necrosis factor alpha (TNF-α), an inflammation-induced cytokine, is involved cell proliferation and differentiation, inflammation and apoptosis. [15] Fantastically, it has been reported that TNF-α can enhance the susceptibility of tumor cells to heat-induced apoptosis by inhibiting heat shock transcription factor-1 (HSF 1) activation, HSP 70 [16] or HSP 27 [17] synthesis. Of great interest are cellular membranes of mature DCs, which play essential roles in priming T cells.

Recently, natural cell membrane-coated nanoparticles have arisen as biomimetic theranostic platform for cancer therapeutic applications. [18] These nanoparticles were

inspired from natural cell membranes structure, which inherit the membrane protein profile of the source cells, enabling them to act as seemingly source cells that can deliver the cargos to the targeting site, meanwhile activate immune-associated cells. The natural cell membrane-coated nanoparticles strike a chord with the concept “Terminators”, the killing machines with living tissue over robotic endoskeleton with organic marital, which inspired us to develop nanoscale “Terminator” for cancer termination. In this work, we developed biomimetic nanoterminator with mature dendritic cell activities (mDC@NIRdots) by coating mature DC membrane on organic dye/polymer nanoparticles (NPs) with near infrared (NIR)-absorbing ability for immuno-priming mild photothermal cancer therapy. Due to the inherent unique property of mature DC membrane, as-prepared nanoterminator could promote T cells to secrete cytokines, overcome heat shock protein-induced thermoresistance for mild photothermal therapy (~42°C) and persist immune system in response to tumors for life-long autoimmunity.

As shown in **Scheme 1**, the mDC@NIRdots was fabricated according to previous reports with slight modifications. Firstly, the dendritic cells were isolated from female BALB/c mice tibias and femurs and cultured with GM-CSF and IL-4 [19]. The maturated DC cells were generated by incubation of immature DC cells with the mixture of tumor antigens and polycytidylic acid (usually abbreviated Poly (I:C)) (**Figure S1)**. As one of the most potent clinical immunostimulants, Poly (I:C) could interact with toll-like receptor 3, which is expressed at the endosomal membrane of dendritic cells. The combination treatment of tumor antigens with Poly (I:C) could

enhance the sensitization ability of tumor antigens and activate dendritic cells maturation [20]. Besides, the tumor antigens could further sensitize DCs for priming of both $CD4^+$ and $CD8^+$ T lymphocytes in vivo [21]. Secondly, the mature DC membranes were undressed from the cells and coated onto NIRdots by extrusion method. iDC@NIRdots (NIRdots coated with un-maturated dendritic cell membrane) were also prepared according to the similar procedure and used as control for the further experiments. As shown in **Figure 1**, the morphology of as prepared mDC@NIRdots was investigated using transmission electron microscopy (TEM). The results indicated that the mDC@NIRdots were in spherical shape with an average size of 92.1±3.8 nm. The cell membranes coating on mDC@NIRdots could also be easily observed with the thickness of 6.9 nm, which was consistent with previous reports (5~10 nm) (**Figure 1A and Figure S2**) [18]. As shown in **Figure 1A**, the hydrodynamic diameter of mDC@NIRdots was measured to be 103.2±4.5 nm using dynamic light scattering (DLS) method, which was ~14.1nm more than that of NIRdots (89.1±3.9 nm, **Figure S3**). The slight increase of hydration diameter was attributed to the cell membrane wrapped on the surface of nanodots, which was consistent with the result of TEM. The membrane protein composition on the mDC@NIRdots surface was analyzed with SDS-PAGE electrophoresis and compared with the original membrane protein composition on the mature DC. As shown in **Figure 1B**, the membrane protein composition of mature DC was successfully implanted on nanoparticles through this biomimetic approach and the mature DC membrane characteristics were well retained. In comparison to NIRdots group, the leakage of IR-797 from

mDC@NIRdots was obviously reduced (**Figure 1C**). To evaluate the stability of mDC@NIRdots, the nanoparticles were dissolved in water, PBS, DMEM and FBS, respectively. After 2 weeks store under room temperature, there were no precipitation occurred in mDC@NIRdots samples **(Figure S4A)**. To assess its hemocompatibility, the different concentration of nanoparticles dissolved in PBS containing red cells. As shown in **Figure S4B**, there was no hemolysis in mDC@NIRdots. These results indicated that mature DC membrane coating improved the stability and biocompatibility of NIRdots. The absorption and the emission spectra of the NIRdots with and without mDC membrane coating were recorded in PBS buffer respectively and compared with the IR-797 molecules measured in water solution (**Figure 1D and 1E**). The mDC@NIRdots solution exhibited an absorption peak at 797 nm which was consistent with the absorbance peak of IR-797. The broaden and red-shifted absorbance of NIRdots and mDC@NIRdots was possibly due to the IR-797 received stronger intermolecular π−π interactions inside the nanoparticles. The emission maximum of mDC@NIRdots and dots appeared at 820 nm with QY ~0.04%, much lower compared with that of free IR-797 (0.25%), which may be due to the aggregation caused quenching (ACQ) effect. We next evaluated the photothermal effect of mDC@NIRdots. Free IR-797 was used as a control. The temperature of mDC@NIRdots solution (5 μg/ml) reached a maximum at ~ 42 °C after 808 nm laser irradiation (0.2 W/cm^2) for 450 seconds, while the temperature of NIRdots and free IR-797 solution (5 μg/ml) reached to ~40 °C and ~31 °C (**Figure 1F, Figure S5**). The photothermal conversion efficiency of mDC@NIRdots (23.72%) was comparable to

that of NIRdots (21.19%) but ~2 times higher than that of free IR-797(10.97%). These results confirmed that ACQ effect of IR-797 could be beneficial for fabrication NIRdots with more highly efficient photo-thermal transition.[22]

To demonstrate the T cell targeting capability of mDC@NIRdots, T cell were incubated with mDC@NIRdots or iDC@NIRdots (NIRdots coated with un-maturated dendritic cell membrane) respectively and recorded by using confocal laser scanning microscopy (CLSM) and flow cytometry. As shown in **Figure 2A**, the T cell treated with mDC@NIRdots for 3 h showed highly red fluorescent signal when compared to those cells treated with the iDC@NIRdots, which indicated that mDC@NIRdots could effectively bounded on the T cell membrane surface. In contrast, there were little signal on T cell incubated with iDC@NIRdots. In addition, the fluorescence intensity of the treated cells was further analyzed by flow cytometry (**Figure S6 and Figure S7**). The flow cytometric analysis results were consistent with the CLSM data, which further confirmed that the mDC@NIRdots could target the T cell with high efficiency. It was proposed that the inherited membrane proteins on the mDC@NIRdots was expected to help the nanoparticles to specifically bind and activate T cells. As shown in **Figure 2B**, the high expression of CD80, CD86, MHCI and MHCII on mDC membranes of mDC@NIRdots were confirmed by western blotting, which were same as the original ones on natural mature. The GAPDH and Na^+/K^+-ATPase α1 were used as internal references (**Figure 2B**). Furthermore, the CD80, CD86, MHCI, and MHCII proteins were added to

block the receptors on the T cells. Compared with the control group, the fluorescence intensity was significantly reduced when CD80, CD86, MHCI, and MHCII proteins were added (**Figure 2C**), and the fluorescence intensity were lowest in the mixed group. These results indicated that mDC@NIRdots bound with T cells through the specific binding between receptors (CD28, T cell receptor, etc) expressed on T cells and ligands-phased on mature DC cell-membranes (such as CD80, CD86, MHCI, MHCII proteins, etc). [12b,13,23]

To further demonstrate whether as prepared mDC@NIRdots could prime T cell in vitro, the T cells were incubated with mDC@NIRdots for 72h. The proliferation of $CD3^+$ T cells were evaluated using the carboxyfluorescein diacetate succinimidyl ester (CFSE)-based assay. [10a] Compared with the control group, the fluorescence intensity of $CD3^+$ T cells in the mDC@NIRdots group was significantly decreased, which suggested that mDC@NIRdots was able to stimulate T cell proliferation (**Figure S8**). In our study, we used CD3/CD28/IL2 as positive control, which were commercially used for in vitro expansion of T cells[10b]. Natural maturate DCs had the function to promote secretin of cytokines from T cell to participate in the anti-tumor process. [12a] We wonder whether as prepared mDC@NIRdots could also activated the T cell to secret cytokines. Three kinds of cytokines, Interleukin 2 (IL-2) [24] (an important cytokine to promote T cell proliferation), tumor necrosis factor a (TNF-α) [25] (an important cytokine to activate cellular immunity), and interferon-γ (IFN-γ) [26] (an important marker to activate innate immunity) in the medium

supernatant were analysed by ELISA after different treatment of T cells. It was found that the amount of TNF-α, IL-2, and IFN-γ were dramatically increased after treating T cells with mDC@NIRdots, which was positively correlated with concentration of nanoparticles and higher than that of NIRdots and iDC@NIRdots group (**Figure 2D, 2E, and S9**). These results indicated that mDC@NIRdots maintained the T cell priming function of natural mature DC cells, which could stimulate the T cells proliferation and promote the T cells to secrete cytokines. We further evaluated the effect of temperature effect on the T cells proliferation (**Figure S10**). The results demonstrated that under the mild temperature (~42°C), the proliferation of T cells was not affected.

It has been reported that cytokines secreted by T cell could further inhibit the expression of heat shock proteins family (HSPs family, such as Hsp27, Hsp70, Hsp90, Hsp105 and HSF1, etc). [16,17] Considering the inhibiting ability of cytokines to HSPs family, we wondered whether the mDC@NIRdots could inhibit the expression of HSPs family of cancer cell by promoting secretin of cytokines from T cell around cancer cells. As shown in **Figure 3A,** the transwell chamber was used to simulate the tumor-immune microenvironment (TIME) in vitro by placing the breast cancer cell line 4T1 in an upper chamber (the pore size ~ 3 μm) of transwell, and $CD3^+$ T cells in the lower chamber. During the incubation, the whole transwell chamber were exposed to 808 nm laser (0.2 W cm^{-2}) and the temperature were maintained at ~42 °C for 15 min after the two cells were co-incubated with nanoparticles for 48h. After further

incubation at 37 °C for 24 h, 4T1 cells and the supernatant were collected for following assay. As shown in **Figure 3B**, the cytokines in the supernatant with different treatments were analysed by using ELISA method. the results showed that the amount of TNF-α, IL-2, and IFN-γ were dramatically increased after treating with mDC@NIRdots, which was not affect by the laser irradiation (0.2 W cm^{-2}) and the mild temperature heating (~42°C). As shown in **Figure 3C,** the HSPs family protein expression of 4T1 cancer cells after different treatment was further studied by western blot, in which glyceraldehyde 3-phosphate dehydrogenase (GAPDH) served as control reference. The results showed that the expressions of HSPs family (Hsp27, Hsp70, HspP0, Hsp105 and HSF1) in the 4T1 cancer cells treated with mDC@NIRdots were dramatically reduced. However, NIRdots almost had no effect on those proteins production, which indicated the cell membrane protein components on mDC@NIRdots played important role on the inhibiting the expression of HSPs. Compared with TNF-α group (the positive control), mDC@NIRdots showed superior inhibiting ability to the expression of HSPs. Immunofluorescence stain imaging（**Figure 3D**）further also confirmed that mDC@NIRdots could significantly decreased the expression of HSPs.

The mild photothermal-immuno synergistic antitumor effects of as-prepared mDC@NIRdots in vitro were further studied. As shown in **Figure 3E** and **S11,** the expression of pro-apoptotic proteins (Bax, caspase-3 and caspase-8) was clearly enhanced in mDC@NIRdots in comparison with NIRdots group upon

irradiation with 808 nm laser. Moreover, the expression of pro-apoptotic proteins in the mDC@NIRdots group was even higher than that of positive group (TNF-α). In contrast, the expression of anti-apoptotic proteins (Bcl-2 and Bcl-xL) in the mDC@NIRdots group was much lower than that of other groups. These results suggested the synergistic antitumor effects of mDC@NIRdots, which could dramatically promote cancer cell apoptosis in tumor-immune microenvironment under NIR light irradiation. Furthermore, the viabilities of treated 4T1 cell were determined using the standard CCK-8 assay (**Figure S12**). The cell viabilities of 4T1 cells incubated with mDC@NIRdots were significantly decreased after the mild hyperthermia treatment (~42 °C). However, the cancer cells incubated with only NIRdots or PBS buffer remained alive and health under the equal condition. These results demonstrated that mDC@NIRdots could dramatically reduce the resistances of cells to heat stresses. The cells apoptosis was further studied using flow cytometry approach. As shown in **Figure 3F,** the 4T1 cancer cells incubated with mDC@NIRdots in the stimulated tumor-immune microenvironment in vitro showed remarkably apoptosis under mild photothermal treatment (~42 °C). The cell apoptosis was also evaluated using living/dead cell staining imaging approach (**Figure S13**). The results showed that the cells in control or NIRdots group were displayed green fluorescence while red fluorescence was only observed in cells treated with mDC@NIRdots group with 808 nm laser irradiation. It has been reported that the Interleukin 2 (IL-2), [27] tumor necrosis

factor a (TNF-α), [28] and interferon-γ (IFN-γ), [29] three main cytokines produced by T cell after activation could enhance apoptotic positive regulatory protein expression (Caspase 3, Caspase8 and Bax), reduce apoptotic negative regulatory protein expression (Bcl-2, Bcl-xL), and further promoted tumor apoptosis. As results, the cytokines produced by T cell activated by mDC@NIRdots in tumor-immune microenvironment could not only inhibit the expression of heat shock proteins, but also promote tumor apoptosis, which synergistically amplified antitumor effect of antitumor efficacy of mild hyperthermia treatment (~42°C).

To further investigate the mild photothermal-immuno synergistic therapy effect of as prepared nanoterminator in vivo, mDC@NIRdots and NIRdots were administered intratumorally into different groups of 4T1-tumor-bearing mice, respectively. The in vivo animal experiment was designed as shown in **Figure 4A**. Firstly, 4T1 tumor cells were inoculated on the right leg of each mouse as primary tumor. 3 days later, a second tumor was inoculated on the left leg of the same mouse as an artificial mimic of metastasis distant tumor. the mice were treated with NIRdots or mDC@NIRdots (20 mg per kg, based on IR-797 weight) through intratumoral injection on the primary tumor. After two days, the primary tumor was irradiated by 808 nm laser (0.2 $W.cm^{-2}$) and maintained with mild temperature (~42°C) for 30 min.

As shown in **Figure 4B** and **4C**, tumour growth process was monitored by measurement of the tumour size every day. Notably, the growth of primary and

distant tumours in mice was significantly delayed after injection of mDC@NIRdots following mild photothermal treatment (~42°C), which indicated the life-long tumor inhibition potential of mild photothermal treatment based on mDC@NIRdots. The mice body weight was also monitored during the treatment every two days to analyse the treatment-induced toxicity. There were no obvious differences in the body weight of mice after treating with mDC@NIRdots and mild photothermal treatment (~42°C) for several days (**Figure 4D**). In vivo toxicity of nanomaterials is always a considerable concern problem, which determine the applications in drug delivery and imaging. [30] To further study whether mDC@NIRdots cause in vivo side toxicity, several major organs of mice in each treatment group were also excised and sectioned for H&E staining at the time point of 3 days after injection of nanoparticles. As shown in **Figure S14**, no noticeable tissue damage and inflammatory lesion could be found in the organs from all the treatment groups of mice. To further investigate the potential toxicology, The liver function indicators including ALT (alanine aminotransferase), AST (aspartate aminotransferase), ALP (alkaline phosphatase)[31], renal function indictors including BUN (blood urea nitrogen) and CRE(creatinine) [32] and blood index values including red blood cell count, platelet count [33] were analysed and there were no significant differences for all treatment groups **(Figure S15)**. All these results further confirmed the excellent in vivo safety and biocompatibility of as prepared mDC@NIRdots.

As shown in **Figure 4E**, the mice treated with mDC@NIRdots + mild PTT (~42°C) lived more than 60 days. However, the mice treated with NIRdots + mild PTT (~42°C) could only survive for no more than 36 days. Interestingly, the mice treated with mDC@NIRdots could even survive for nearly 40 days. This phenomenon was possible due to the inherent mature DC characteristics of the mDC@NIRdots, which stimulate the whole immune system of the mice. However, only the combination of laser irradiation and mDC@NIRdots could greatly improve and prolong the survival of the mice.

The mechanism of photothermal-immune synergistic therapy using mDC@NIRdots was further studied. The infiltration of $CD8^+$ and $CD4^+$ T cells in the primary tumor, which regulated or assisted in immune response by secreting cytokines, were analysed by flow cytometry at 7 days after mDC@NIRdots treatment. The mDC@NIRdots groups could significantly increase the percentage and number of activated $CD8^+$ and $CD4^+$ T cells in tumor collected from mice compared to other groups (**Figure 5A and B**). Similarly, higher percentage and number of $CD8^+$ and $CD4^+$ T cells were detected in distant tumor after the mDC@NIRdots treatment (**Figure 5C and D**). As shown in **Figure 5E**, the immunofluorescence stain results were consistent with flow cytometry data, which further confirm the T cell activating ability of mDC@NIRdots.

Cytokines secretion in TIME also played an important role in the process of immune anti-tumour responses. [34] The serum of 4T1 tumors-bearing mice were

collected at 24 h, 72 h, 120 h and 168h respectively to detect the variation of several cytokines including TNF-α, IFN-γ, IL-2 and IL-12p70. As shown in **Figure 5F, 5G, S16**, and **S17**, intratumoral injection of mDC@NIRdots was able to increase the pro-inflammatory cytokines (TNF-α, IFN-γ, IL-2 and IL-12p70) secretion, which obviously higher and persistently longer than other groups, which was beneficial to trigger anti-tumor immune response of the whole body. These results demonstrated that the mDC@NIRdots could act as artificial mature dendritic cell in combination with mild hypothermia therapy for potentially tumor termination.

In summary, we developed a mature dendritic cell-like biomimetic nanoterminator mDC@NIRdots for tumor termination under safe and mild temperature conditions (~42°C). This nanoterminator could automatically located on T cell in the TIME and prime T cell for Cytokines secretion, which could not only inhibit the expression of heat shock proteins to accomplish highly efficient mild photothermal therapy (~42°C), but also promote tumour apoptosis during the treatment. More importantly, this nanoterminator could serve as vaccine to trigger anti-tumor immune response of the whole body, which would be promising to long-life tumour inhibition and termination.

Supporting Information

Methods and materials, Supplementary Figures S1-S17. Supporting Information is available from the Wiley Online Library or from the author.

Acknowledgements
This work was supported by Special Research Assistant Project of the Chinese Academy of Sciences (Y959101001), the National Natural Science Foundation of China (31571013, 81671758 and 81901906), Guangdong Natural Science Foundation of Research Team (2016A030312006), Shenzhen Science and Technology Program (JCYJ20160429191503002)

Received: ((will be filled in by the editorial staff))
Revised: ((will be filled in by the editorial staff))
Published online: ((will be filled in by the editorial staff))

References

[1] a) K. A. Cronin, A. J. Lake, S. Scott, R. L. Sherman, A. M. Noone, N. Howlader, S. J. Henley, R. N. Anderson, A. U. Firth, J. Ma, B. A. Kohler, A. Jemal, *Cancer* **2018**; b) J. Candido, T. Hagemann, *J Clin Immunol* **2013**, 33 Suppl 1, S79.
[2] a) A. R. Rastinehad, H. Anastos, E. Wajswol, J. S. Winoker, J. P. Sfakianos, S. K. Doppalapudi, M. R. Carrick, C. J. Knauer, B. Taouli, S. C. Lewis, A. K. Tewari, J. A. Schwartz, S. E. Canfield, A. K. George, J. L. West, N. J. Halas, *Proc Natl Acad Sci U S A* **2019**, 116, 18590; b) J. J. Hu, Y. J. Cheng, X. Z. Zhang, *Nanoscale* **2018**, 10, 22657; c) J. Lin, M. Wang, H. Hu, X. Yang, B. Wen, Z. Wang, O. Jacobson, J. Song, G. Zhang, G. Niu, P. Huang, X. Chen, *Adv Mater* **2016**, 28, 3273.
[3] a) X. Huang, I. H. El-Sayed, W. Qian, M. A. El-Sayed, *J Am Chem Soc* **2006**, 128, 2115; b) Z. Zhao, C. Chen, W. Wu, F. Wang, L. Du, X. Zhang, Y. Xiong, X. He, Y. Cai, R. T. K. Kwok, J. W. Y. Lam, X. Gao, P. Sun, D. L. Phillips, D. Ding, B. Z. Tang, *Nat Commun* **2019**, 10, 768.
[4] a) X. Zhu, W. Feng, J. Chang, Y. W. Tan, J. Li, M. Chen, Y. Sun, F. Li, *Nat Commun* **2016**, 7, 10437; b) W. H. Chen, G. F. Luo, Q. Lei, S. Hong, W. X. Qiu, L. H. Liu, S. X. Cheng, X. Z. Zhang, *ACS Nano* **2017**, 11, 1419; c) L. Huang, Y. Li, Y. Du, Y. Zhang, X. Wang, Y. Ding, X. Yang, F. Meng, J. Tu, L. Luo, C. Sun, *Nat Commun* **2019**, 10, 4871; d) Y. Cao, T. Wu, K. Zhang, X. Meng, W. Dai, D. Wang, H. Dong, X. Zhang, *ACS Nano* **2019**, 13, 1499.
[5] a) S. Wang, Y. Tian, W. Tian, J. Sun, S. Zhao, Y. Liu, C. Wang, Y. Tang, X. Ma, Z. Teng, G. Lu, *ACS Nano* **2016**, 10, 8578; b) K. Zhang, X. D. Meng, Y. Cao, Z. Yang, H. F. Dong, Y. D. Zhang, H. T. Lu, Z. J. Shi, X. J. Zhang, *Adv. Funct. Mater*. **2018**, 28, 10.

[6] a) K. Palucka, J. Banchereau, *Nat Rev Cancer* **2012**, 12, 265; b) K. Y. Helmy, S. A. Patel, G. R. Nahas, P. Rameshwar, *Ther Deliv* **2013**, 4, 1307; c) M. H. Kershaw, M. W. Teng, M. J. Smyth, P. K. Darcy, *Nat Rev Immunol* **2005**, 5, 928; d) M. S. Goldberg, *Nat Rev Cancer* **2019**, 19, 587.
[7] M. D. Gholami, G. A. Kardar, Y. Saeedi, S. Heydari, J. Garssen, R. Falak, *Cell Immunol* **2017**, 322, 1.
[8] K. E. Pauken, E. J. Wherry, *Trends in Immunology* **2015**, 36, 265.
[9] D. Li, X. Li, W. L. Zhou, Y. Huang, X. Liang, L. Jiang, X. Yang, J. Sun, Z. Li, W. D. Han, W. Wang, *Signal Transduct Target Ther* **2019**, 4, 35.
[10] a) Q. Chen, Q. Hu, E. Dukhovlinova, G. Chen, S. Ahn, C. Wang, E. A. Ogunnaike, F. S. Ligler, G. Dotti, Z. Gu, *Adv. Mater.* **2019**, 31; b) A. S. Cheung, D. K. Y. Zhang, S. T. Koshy, D. J. Mooney, *Nat Biotechnol* **2018**, 36, 160.
[11] a) M. Ferrantini, I. Capone, F. Belardelli, *Cytokine Growth F R* **2008**, 19, 93; b) A. Gardner, B. Ruffell, *Trends Immunol* **2016**, 37, 855.
[12] a) S. Hao, O. Bai, F. Li, J. Yuan, S. Laferte, J. Xiang, *Immunology* **2007**, 120, 90; b) J. E. Jang, C. H. Hajdu, C. Liot, G. Miller, M. L. Dustin, D. Bar-Sagi, *Cell Rep* **2017**, 20, 558.
[13] a) T. Shin, G. Kennedy, K. Gorski, H. Tsuchiya, H. Koseki, M. Azuma, H. Yagita, L. Chen, J. Powell, D. Pardoll, F. Housseau, *J Exp Med* **2003**, 198, 31; b) T. J. Thauland, Y. Koguchi, M. L. Dustin, D. C. Parker, *J Immunol* **2014**, 193, 5894.
[14] D. Torralba, N. B. Martin-Cofreces, F. Sanchez-Madrid, *Immunol Lett* **2019**, 209, 11.
[15] R. van Horssen, T. L. Ten Hagen, A. M. Eggermont, *Oncologist* **2006**, 11, 397.
[16] G. Schett, C. W. Steiner, Q. Xu, J. S. Smolen, G. Steiner, *Cell Death Differ* **2003**, 10, 1126.
[17] M. Niwa, K. Hotta, A. Hara, K. Hirade, H. Ito, K. Kato, O. Kozawa, *Life Sci* **2006**, 80, 181.
[18] a) C. M. Hu, R. H. Fang, K. C. Wang, B. T. Luk, S. Thamphiwatana, D. Dehaini, P. Nguyen, P. Angsantikul, C. H. Wen, A. V. Kroll, C. Carpenter, M. Ramesh, V. Qu, S. H. Patel, J. Zhu, W. Shi, F. M. Hofman, T. C. Chen, W. Gao, K. Zhang, S. Chien, L. Zhang, *Nature* **2015**, 526, 118; b) A. V. Kroll, R. H. Fang, Y. Jiang, J. Zhou, X. Wei, C. L. Yu, J. Gao, B. T. Luk, D. Dehaini, W. Gao, L. Zhang, *Adv Mater* **2017**, 29, 1703969; c) D. Dehaini, X. Wei, R. H. Fang, S. Masson, P. Angsantikul, B. T. Luk, Y. Zhang, M. Ying, Y. Jiang, A. V. Kroll, W. Gao, L. Zhang, *Adv Mater* **2017**, 29, 1606209; d) Y. Zou, Y. Liu, Z. Yang, D. Zhang, Y. Lu, M. Zheng, X. Xue, J. Geng, R. Chung, B. Shi, *Adv Mater* **2018**, 30, e1803717; e) W. L. Liu, M. Z. Zou, T. Liu, J. Y. Zeng, X. Li, W. Y. Yu, C. X. Li, J. J. Ye, W. Song, J. Feng, X. Z. Zhang, *Adv Mater* **2019**, 31, e1900499; f) C. Luo, X. Hu, R. Peng, H. Huang, Q. Liu, W. Tan, *ACS Appl Mater Interfaces* **2019**, in press; g) G. J. Deng, Z. H. Sun, S. P. Li, X. H. Peng, W. J. Li, L. H. Zhou, Y. F. Ma, P. Gong, L. T. Cai, *ACS Nano* **2018**, 12, 12096; h) L. Rao, L. L. Bu, Q. F. Meng, B. Cai, W. W. Deng, A. Li, K. Y. Li, S. S. Guo, W. F. Zhang, W. Liu, Z. J. Sun, X. Z. Zhao, *Adv. Funct. Mater*. **2017**, 27, 1604774; i) J. Z. Lai, G. J. Deng, Z. H. Sun, X. H. Peng, J. Li, P. Gong, P. F. Zhang, L. T. Cai, *Biomaterials* **2019**,

211, 48; h) P. Zhang, L. Zhang, Z. Qin, S. Hua, Z. Guo, C. Chu, H. Lin, Y. Zhang, W. Li, X. Zhang, X. Chen, G. Liu, *Adv Mater* **2018**, 30, e1705350.
[19] a) Y. Xu, Y. Zhan, A. M. Lew, S. H. Naik, M. H. Kershaw, J Immunol 2007, 179, 7577; b) K. Inaba, M. Inaba, N. Romani, H. Aya, M. Deguchi, S. Ikehara, S. Muramatsu, R. M. Steinman, *J Exp Med* **1992**, 176, 1693.
[20] J. Fucikova, D. Rozkova, H. Ulcova, V. Budinsky, K. Sochorova, K. Pokorna, J. Bartunkova, R. Spisek, *J Transl Med* **2011**, 9, 223.
[21] A. Regnault, D. Lankar, V. Lacabanne, A. Rodriguez, C. Thery, M. Rescigno, T. Saito, S. Verbeek, C. Bonnerot, P. Ricciardi-Castagnoli, S. Amigorena, *J Exp Med* **1999**, 189, 371.
[22] a) W. Hu, X. Miao, H. Tao, A. Baev, C. Ren, Q. Fan, T. He, W. Huang, P. N. Prasad, *ACS Nano* **2019**, 13, 12006; b) W. Lin, Y. Li, W. Zhang, S. Liu, Z. Xie, X. Jing, *ACS Appl Mater Interfaces* **2016**, 8, 24426.
[23] D. Rea, F. H. Schagen, R. C. Hoeben, M. Mehtali, M. J. Havenga, R. E. Toes, C. J. Melief, R. Offringa, *J Virol* **1999**, 73, 10245.
[24] R. A. Rosalia, N. Arenas-Ramirez, G. Bouchaud, M. E. Raeber, O. Boyman, *Curr Opin Chem Biol* **2014**, 23, 39.
[25] a) R. van Horssen, T. L. Ten Hagen, A. M. Eggermont, *Oncologist* **2006**, 11, 397; b) B. L. Salomon, M. Leclerc, J. Tosello, E. Ronin, E. Piaggio, J. L. Cohen, Front *Immunol* **2018**, 9, 444.
[26] a) C. F. Lin, C. M. Lin, K. Y. Lee, S. Y. Wu, P. H. Feng, K. Y. Chen, H. C. Chuang, C. L. Chen, Y. C. Wang, P. C. Tseng, T. T. Tsai, *J Biomed Sci* **2017**, 24, 10; b) J. Xiang, L. G. Xu, H. Gong, W. W. Zhu, C. Wang, J. Xu, L. Z. Feng, L. Cheng, R. Peng, Z. Liu, *ACS Nano* **2015**, 9, 6401.
[27] a) Y. Darif, D. Mountassif, A. Belkebir, Y. Zaid, K. Basu, W. Mourad, M. Oudghiri, *J Toxicol Sci* **2016**, 41, 403; b) M. Zhang, L. A. Mathews Griner, W. Ju, D. Y. Duveau, R. Guha, M. N. Petrus, B. Wen, M. Maeda, P. Shinn, M. Ferrer, K. D. Conlon, R. N. Bamford, J. J. O'Shea, C. J. Thomas, T. A. Waldmann, *Proc Natl Acad Sci U S A* **2015**, 112, 12480.
[28] a) M. Ghandadi, J. Behravan, K. Abnous, M. Ehtesham Gharaee, F. Mosaffa, *Cytokine* **2017**, 97, 167; b) K. Mizrahi, J. Stein, I. Yaniv, O. Kaplan, N. Askenasy, *Stem Cells* **2013**, 31, 156.
[29] a) Z. H. Cao, W. D. Yin, Q. Y. Zheng, S. L. Feng, G. L. Xu, K. Q. Zhang, *Cell Biochem Biophys* **2013**, 67, 1239; b) S. Hacker, A. Dittrich, A. Mohr, T. Schweitzer, S. Rutkowski, J. Krauss, K. M. Debatin, S. Fulda, *Oncogene* **2009**, 28, 3097.
[30] a) T. Kang, Q. Zhu, D. Wei, J. Feng, J. Yao, T. Jiang, Q. Song, X. Wei, H. Chen, X. Gao, J. Chen, *ACS Nano* **2017**, 11, 1397. b) E. Perez-Herrero, A. Fernandez-Medarde, *Eur J Pharm Biopharm* **2015**, 93, 52.
[31] Q. Cheng, T. Wei, Y. Jia, L. Farbiak, K. Zhou, S. Zhang, Y. Wei, H. Zhu, D. J. Siegwart, *Adv Mater* **2018**, 30, e1805308.
[32] Y. Xu, B. Zhang, D. Xie, Y. Hu, H. L. Li, L. L. Zhong, H. W. Wang, W. Jiang, Z. P. Ke, D. H. Zheng, *Oncotarget* **2017**, 8, 39547.
[33] Q. Chen, L. Xu, C. Liang, C. Wang, R. Peng, Z. Liu, *Nat Commun* **2016**, 7, 13193.

[34] a) J. Galon, A. Costes, F. Sanchez-Cabo, A. Kirilovsky, B. Mlecnik, C. Lagorce-Pages, M. Tosolini, M. Camus, A. Berger, P. Wind, F. Zinzindohoue, P. Bruneval, P. H. Cugnenc, Z. Trajanoski, W. H. Fridman, F. Pages, *Science* **2006**, 313, 1960; b) T. R. Mosmann, *Int Arch Allergy Appl Immunol* **1991**, 94, 110.

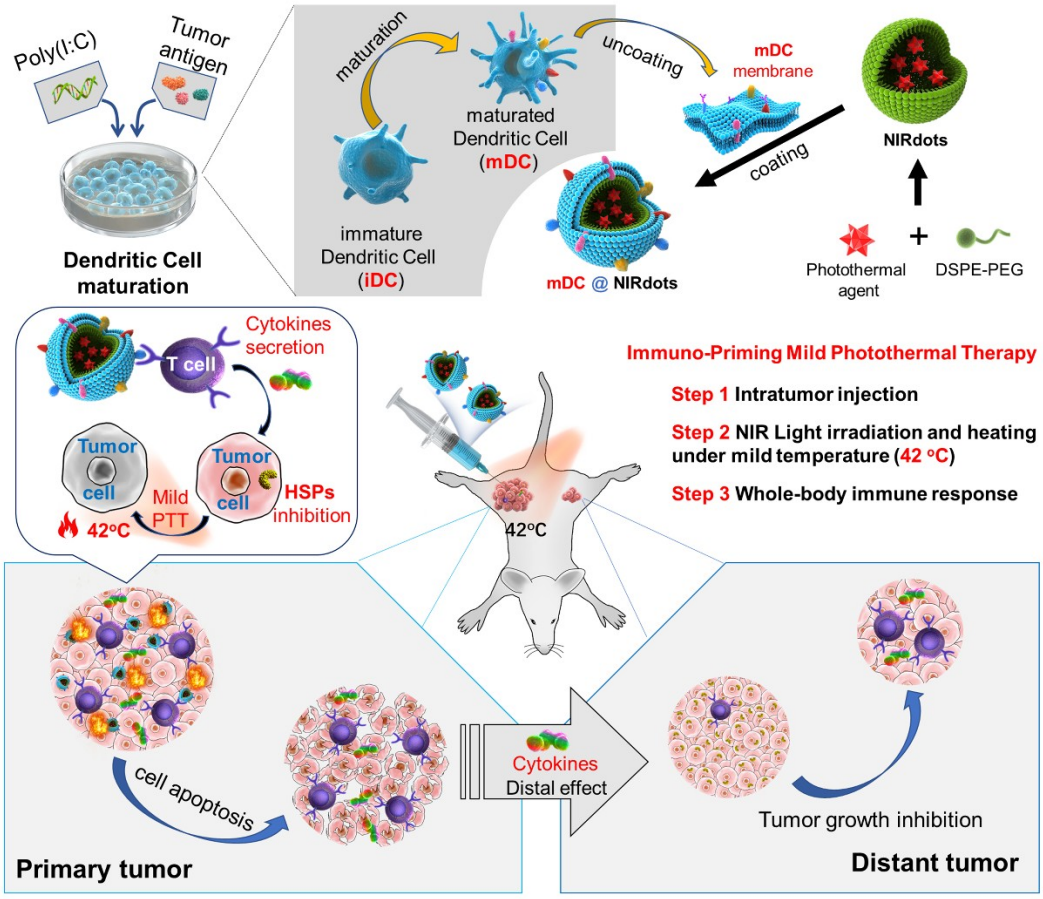

Scheme 1. Schematic illustration of preparation of biomimetic nanoterminators (mDC@NIRdots) for mild photothermal-immuno synergistic therapy. The mDC@NIRdots with mature DCs functions was produced by coating natural mature DC membrane on organic dye/polymer nanoparticles (NPs) with near infrared (NIR)-absorbing ability. When the nanoterminators were injected into tumor-immune microenvironment, they could automatically locate on T cell and promote the T cells enrichment, proliferation, activation and cytokine secretion. The produced cytokines could not only inhibit the expression of heat shock proteins to cooperate on highly efficient mild photothermal therapy (~42°C), but also promote tumor apoptosis during the treatment. mDC@NIRdots could further trigger anti-tumor immune response of the whole body for longlife tumor inhibition and termination.

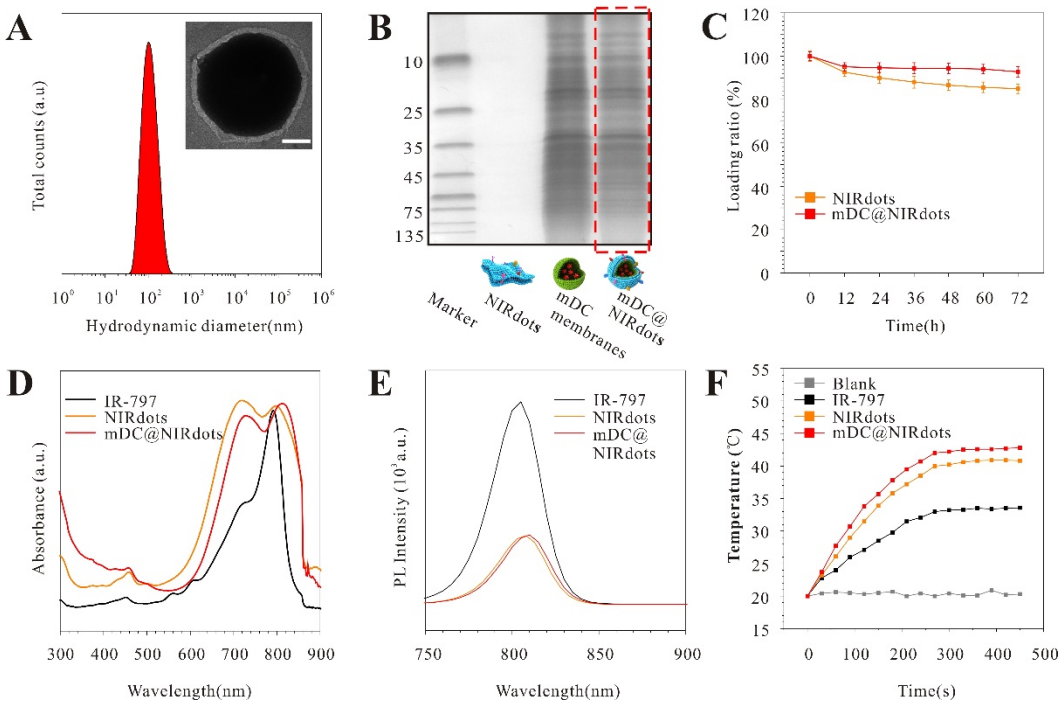

Figure 1. Characterization of mDC@NIRdots. (A) The dynamic light scattering (DLS) measurement results of mDC@NIRdots. Inset: TEM image of mDC@NIRdots. (B) Cell membrane protein on mDC@NIRdots evaluated by SDS-PAGE. DC cell membrane vesicles were used as control. (C) The stability test of mDC@NIRdots. NIRdots were used as control. Data were presented as mean ± s.d. (*n* = 5). (D) The absorbance spectrum of IR-797, NIRdots and mDC@NIRdots, respectively. (E) The fluorescence spectra of IR-797, NIRdots and mDC@NIRdots. (g) The temperature change of IR-797, NIRdots and mDC@NIRdots under the 808nm laser (0.2 Wcm^2) irradiation for 8 min, respectively. PBS buffer was used as control.

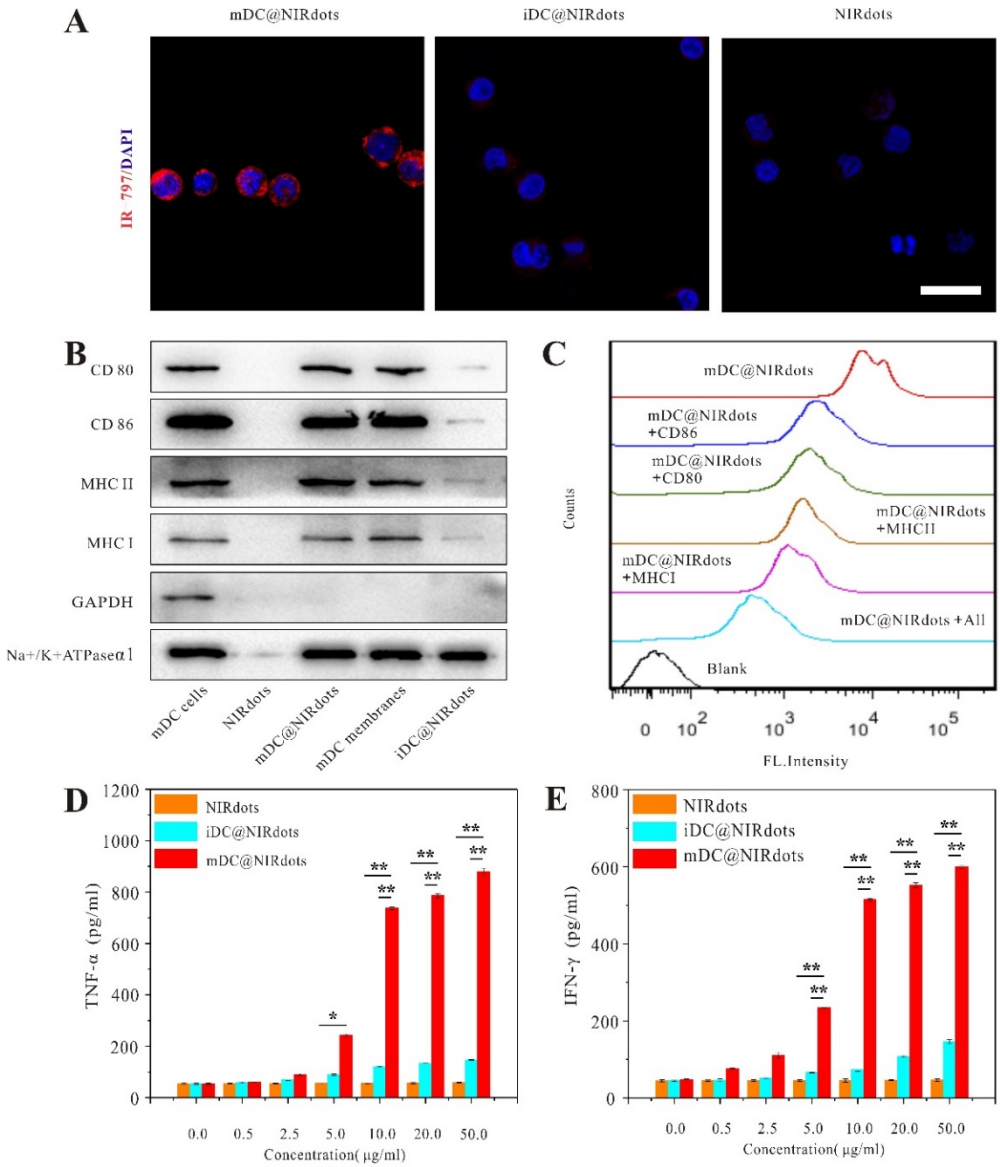

Figure 2. In vitro investigate the ability of mDC@NIRdots specifically bind to T cells and activation of T cells. (A) mDC@NIRdots bound on the cell membrane of $CD3^+$T cells. mDC@NIRdots (10μg/ml, IR-797 weight) or NIRdots (10μg/ml, IR-797 weight) or iDC@NIRdots (10μg/ml, IR-797 weight) were incubated with $CD3^+$T cells for 3 h. IR-797 (red color) were used to detect the NPs on $CD3^+$ T cells membrane. DAPI (blue color) were used to detect the nucleus of $CD3^+$ T cells (Scar bar: 25 μm). (B) Western blot was used to examine the T cell activation associated protein of mDC@NIRdots. The protein signals of GAPDH and Na^+/K^+-ATPase α1 served as control. CD80, CD86, MHC I and MHC II were the key protein for T cell activation. (C) Flow cytometry analysis of mDC@NIRdots binding with $CD3^+$ T cells after indication with the CD80, CD86, MHC I and MHC II proteins for 3 h. (D) and (E) ELISA was used to analysis the cytokines. $CD3^+$ T cells were treated with mDC@NIRdots or NIRdots or iDC@NIRdots with varied concentrations, and the secreted cytokines concentrations of TNF-α (D) and IFN-γ (E) in culture media were measured after incubation 72 h (n = 3). Error bar, mean ± s.d. P value: *P < 0.05, **P < 0.01.

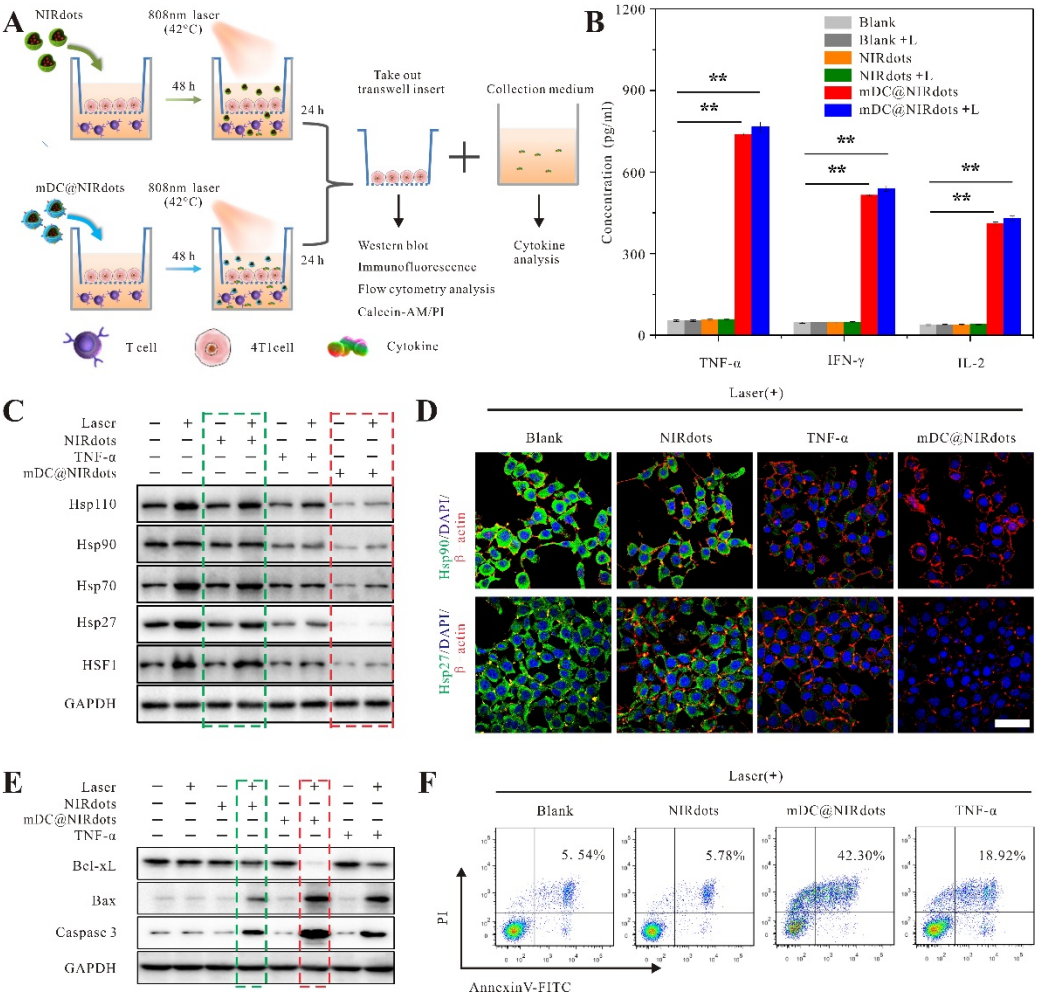

Figure 3. In vitro anti-tumor effect of mDC@NIRdots (A)Schematic illustration of mDC@NIRdots and NIRdots treatment processing. (B) The cytokines analysis after different treatments. $CD3^{+}$T cells were treated with mDC@NIRdots(10μg/ml) or NIRdots (10μg/ml) or PBS for 48h, and irradiation for 30 min at 42 °C and then cultured at 37 °C for 24 h, the concentrations of TNF-α, IFN-γ and IL-2 in culture media were measured (n = 3). Error bar, mean ± s.d. P value: *P < 0.05, **P < 0.01. (C) After different treatment, the HSPs protein expression were detected by Western blot with GADPH as an internal reference. (D) Confocal fluorescence images showed the Hsp90 and Hsp27 expression.(E) Western blot images were used to detect the apoptosis protein maker with GADPH as an internal reference, for cell lysates of 4T1 cells after various treatments. (F) Flow cytometry analysis of mDC@NIRdots (10μg/ml) or NIRdots (10μg/ml) or PBS with and without laser irradiation treatment (42°C) induced apoptosis with Annexin V-FITC and PI.

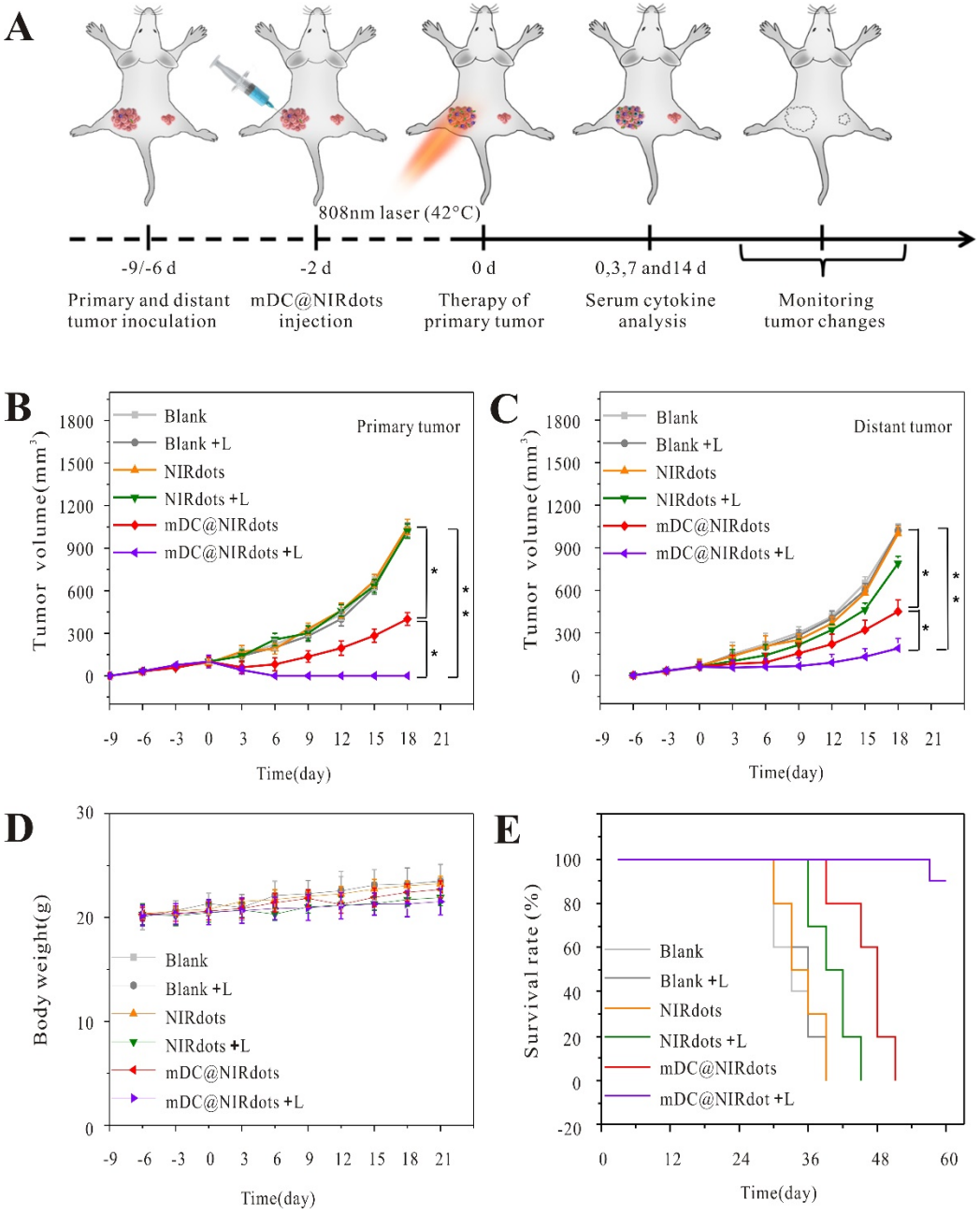

Figure 4. In vivo anti-tumour effect of mDC@NIRdots based PTT and the mechanism study. (A) Schematic illustration of mDC@NIRdots based PTT to inhibit tumour growth at primary and distant sites. (B), (C) Primary and distant tumour growth curves of the treated mice in different groups (10 mice per group) Error bar, mean ± s.d. *P* value: **P* < 0.05, ***P* < 0.01. (D) Body weights of mice received the different treatment. Error bar, mean ± s.d. (E) Survival curves for the mice received the treatment of mDC@NIRdots, NIRdots, and PBS with or without laser irradiation (*n* = 10).

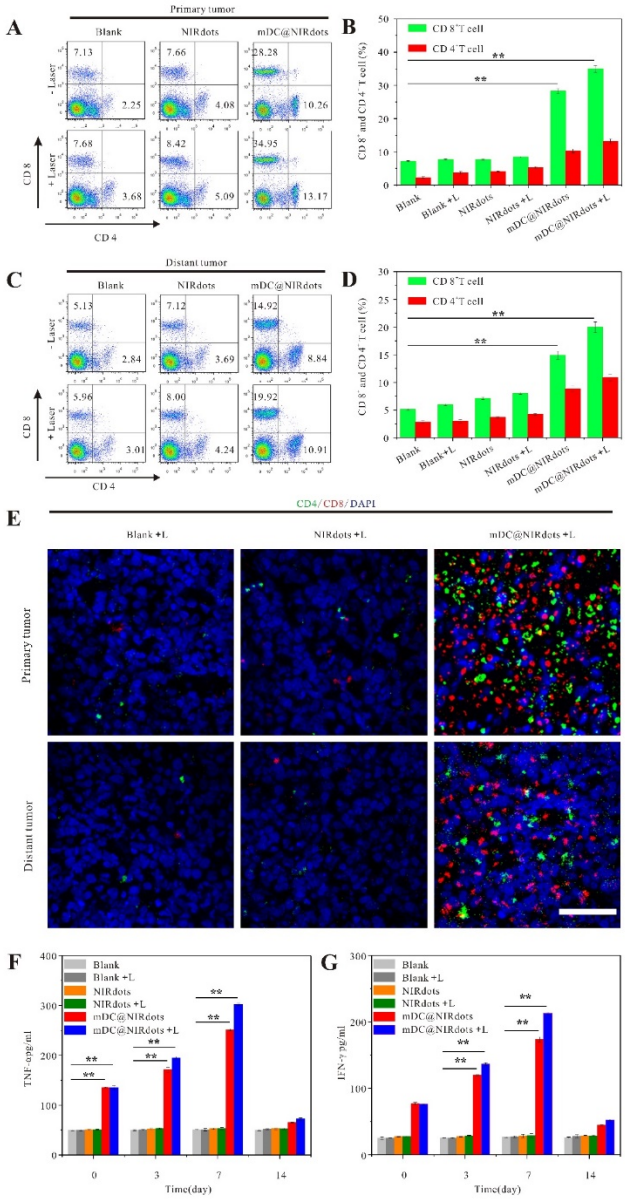

Figure 5. In vivo anti-tumour mechanism study of mDC@NIRdots. (A), (B) Representative flow cytometry plots and quantitative analysis showing the T cells of primary tumours in different groups. After various treatments for 7 days, tumor cell suspensions were collected and analyzed by flow cytometry for T-cell infiltration (gated on $CD3^+$ T cells) (n = 3) Error bar, mean ± s.d. (C), (D) Representative flow cytometry plots and quantitative analysis showing the T cells of disatnt tumours in different groups. After various treatments for 7 days, tumor cell suspensions were collected and analyzed by flow cytometry for T-cell infiltration (gated on $CD3^+$ T cells). (E) Representative immunofluorescence imaging in the primary and distant tumor sections showing infiltrated $CD4^+$ T cells and $CD8^+$ T cells. The tumour were collected after different treatments for 7 days. Scar bar: 50 μm. Murine TNF-α(F) and IFN-γ (G)levels detected at day 0, 3, 7, 14 after indicated treatments (n = 3). Error bar, mean ± s.d. P value: *P < 0.05, **P < 0.01.

The NIR nanoterminators with mature Dendritic Cell functions were developed to locating on T cell in the complex tumor-immune microenvironment automatically and promote the T cells proliferation, activation and cytokine secretion, inhibiting the expression of heat shock proteins to cooperate on highly efficient mild photothermal therapy (~42°C) and promoting tumor apoptosis and long-life inhibition.

Keyword NIR, mild photothermal therapy, mature dendritic cells, tumor-immune microenvironment, biomimetic theranostics

Zhihong Sun‡, Guanjun Deng‡, Xinghua Peng ‡, Xiuli Xu, Lanlan Liu, Zhen Xu, Yifan Ma, Pengfei Zhang,* Ping Gong,* and Lintao Cai*

NIR Nanoterminator with Mature Dendritic Cell Acitivities for Immuno-Priming Mild Photothermal Cancer Therapy

ToC figure ((Please choose one size: 55 mm broad × 50 mm high **or** 110 mm broad × 20 mm high. Please do not use any other dimensions))

TOC figure